Article

Journal of
Biomedical Nanotechnology
Vol. 20, 655–666, 2024
www.aspbs.com/jbn

Folate Receptor-Targeted Nanodelivery of Apigenin in Breast Cancer: Formulation Development, Characterization and *In Vitro* Evaluation

Arjun Patra[1, 2], Swaha Satpathy[1, $], Pradeep K. Naik[3], Mohsin Kazi[4], and Muhammad Delwar Hussain[5, *]

[1] *Department of Pharmaceutical & Biomedical Sciences, College of Pharmacy, California Health Sciences University, Clovis, 93612, California, USA*
[2] *Department of Pharmacy, Guru Ghasidas University, Bilaspur, 495009, Chhattisgarh, India*
[3] *Department of Biotechnology and Bioinformatics, Sambalpur University, Burla, 768019, Sambalpur, Odisha, India*
[4] *Department of Pharmaceutics, College of Pharmacy, King Saud University, P.O. Box 2457, Riyadh, 11451, Saudi Arabia*
[5] *Department of Pharmaceutical Sciences, School of Pharmacy and Health Professions, University of Maryland Eastern Shore, Princess Anne, MD, 21853, USA*

Cancer is a dreadful disease with a high mortality rate and breast cancer is the most common cancer among females in the world. Different strategies have been used for the treatment of breast cancer, including chemotherapy but it has a wide range of side effects. This problem can be overcome by delivering anticancer agents with nano-formulations. Apigenin (4′,5,7-trihydroxyflavone), present in many different medicinal plants, shows potential anticancer properties in various cancers. However, its use in clinical practice is limited due to its low water solubility and bioavailability. In this study, we examined folate receptor-targeted and PEGylated poly(lactide-co-glycolide) nanoparticles (PLGA-PEG-FA NPs) containing apigenin for targeted delivery to MCF-7 breast cancer cells. Apigenin-loaded PLGA-PEG and PLGA-PEG-FA NPs were small in size, had a negative zeta potential, showed sustained release of apigenin and showed significantly higher anticancer activity than the free drug in breast cancer cells. The half maximal inhibitory concentration (IC_{50}) values of apigenin, apigenin-loaded PLGA, PLGA-PEG and PLGA-PEG-FA NPs were 50.2, 49.4, 18.1 and 13.3 μM, respectively. Apigenin-loaded PLGA-PEG and PLGA-PEG-FA NPs showed 2.79- and 3.77-fold higher cytotoxicity than the pristine drug. Folate-conjugated PLGA nanoparticles could be developed for potential target-specific delivery of apigenin in the treatment of breast cancer.

KEYWORDS: *Apigenin, Breast Cancer, Folate Receptor Targeting, PLGA.*

INTRODUCTION

Globally, the mortality and morbidity due to cancer is rising daily, and according to the World Health Organization (WHO) the number of new cancer cases will be approximately 22 million in the next two decades compared to 14 million in 2012. It has been observed that the common cancer types vary by geographical area, but breast cancer is most commonly diagnosed in females in all regions [1, 2]. Various therapeutic strategies, such as surgery, radiation, biological therapy, and chemotherapy have been used for cancer management. Patients undergoing chemotherapy have an enhanced survival rate, but chemotherapy have unpredictable bioavailability, fast metabolism, serious side effects, non-specific distribution, and toxic effects. These limitations could be overcome by targeted delivery of the anticancer agents specifically to cancer cells with no/less harm to normal cells.

Nano drug delivery systems have immensely contributed to the field of cancer treatment, as various nanoparticle formulations of anticancer agents have been employed for target-specific delivery with passive and/or active targeting. Polymeric nanoparticles (NPs) provide efficient advantages such as enhanced therapeutic activity and reduced side effects compared to conventional cancer

*Author to whom correspondence should be addressed.
Email: mdhussain@umes.edu
$Current address: Raigarh College of Pharmacy, Raigarh, Chhattisgarh, India
Received: 23 August 2023
Accepted: 16 October 2023

therapies [3, 4]. Poly(lactic-co-glycolic acid) (PLGA), a biodegradable and biocompatible polymer, has been approved by the US Food Drug Administration (USFDA) and European Medicine Agency (EMA) for various biomedical applications, including formulation development for cancer treatment. The enhanced permeability and retention (EPR) effect, passive targeting (due to the size, shape and surface charge of NPs), active targeting (because of attached ligands on the NPs), sustained drug release, and increased drug deposition in tumor vasculature can be fulfilled by the application of PLGA NPs [5, 6]. NP formulations with both active and passive targeting properties are desirable in cancer treatment because they produce enhanced cellular uptake [4, 7].

Specificity of a formulation/drug towards cancer cells has been achieved by various active targeting of receptors that are overexpressed on some human cancer cell lines [8]. Folic acid receptor or folate receptor (FR) is overexpressed in different cancer cells, including breast cancer cells [9, 10]. Different targeting ligands have been used for novel drug development in cancer therapy, but folic acid (FA) has been extensively employed due to various advantages, such as (1) low cost, (2) easy availability, (3) stability in processing and storage, (4) non-immunogenic, (5) high binding affinity (10^{-10} M), and (6) simple conjugation to other molecules through its carboxyl group [11, 12]. The FA-conjugated targeted delivery approach has enhanced the anticancer potential of a number of anticancer agents in comparison to the free drug [12]. Of the three subtypes of FRs (FRα, FRβ and FRγ), FRα is a glycosylphosphatidylinositol-anchored membrane glycoprotein and is overexpressed in different cancer cells, including breast cancer cells. FRβ is also overexpressed on cancer cells, but FRα has high affinity for circulating folic acid coenzymes and physiological FA compared to FRβ [13]. FRα is highly expressed in cancer cells, as it is required for rapid and uncontrolled growth, and less expressed in normal human cells [14]. Hence, FRα is considered the predominant targeting receptor for FA-decorated drug carriers for cancer therapy [12]. Folate receptor targeting in cancer treatment mainly involves delivery of anticancer agents as nanodelivery systems with active and passive targeting, and development of folate receptor-targeted imaging agents for detection/diagnosis of cancer. This technology has been employed for diagnosis and treatment of cancers affecting women including breast cancer [15]. A number of novel drug delivery systems such as nanoparticle conjugates, micelles, dendrimers, liposomes, emulsions and nanogels have been adopted for effective cancer therapeutics through folate receptor targeting [16, 17].

Herbal medicines in the form of raw drugs, extracts, fractions, isolated phytoconstituents or different dosage forms are gaining substantial interest because of their beneficial role in the treatment of various ailments, including cancer. Research in the field of cancer treatment with chemopreventive, antioxidant and anti-inflammatory bioactive molecules from natural sources is tremendously increasing [18]. Many plant-derived anticancer agents play pivotal roles in the management of cancer by inhibiting invasion and metastasis [19]. Natural anticancer molecules such as paclitaxel [20], 5-fluorouracil [21], genistein [22], capecitabin [23], 17-allylamino-17-demethoxygeldanamycin [10], vincristine [24], artemether [25] have been delivered as folate receptor targeted nanodelivery system, where they exhibited significantly higher cytotoxicity than the pristine drug.

Apigenin (4′,5,7-trihydroxyflavone) (Fig. 1), a natural flavonoid, is effective against different types of cancer, including breast cancer [18, 26–28]. Apigenin is abundantly available in commonly used fruits, vegetables and green leaves apart from other medicinal plants. It shows anticancer properties by modulating various targets, such as like PI3K/AKT/mTOR, JAK/STAT, NF-κB, MAPK/ERK, and Wnt/β-catenin, and regulating various cell signaling pathways for the development and expansion of cancer [18, 29–31]. Apigenin showed *in vitro* cytotoxicity in a range of breast cancer cell lines, such as MCF-7, T47D, MDA-MB-231, MDA-MB-436, MCF-7/ADR, ZR75.1, MDA-MB-468, 4T1, Hs578T, BT-474, SKBR3, MCF-10A, MDA-MB-268, MDA-MB-453, and HBL-100. The molecular mechanisms of the anticancer activity of apigenin against different cancer types, including breast cancer has been summarized recently by Ahmed et al. [18]. Apigenin modulated various hallmarks of cancer like metastasis, cell proliferation, apoptosis, autophagy, cell cycle arrest etc. by regulating various cell signalling pathways of cancer progression [18]. Despite its of potent anticancer activity, the application of apigenin is limited due to its low lipid solubility (0.001–1.63 mg/mL in nonpolar solvents) and water solubility (2.16 μg/mL), and bioavailability [32–34]. Furthermore, flavonoids including apigenin could be degraded in acidic and alkaline conditions by hydrolysis [35]. To overcome this problem, apigenin has been fabricated as different nano-formulations, which have increased its anticancer properties against various cancer cells [36–39]. However, the advantages of the nanocarrier system, PEGylation and targeted delivery in a single preparation have not been employed to fabricate a formulation against breast cancer. Therefore, the main objective of the present investigation was the development of a nanodelivery system for apigenin

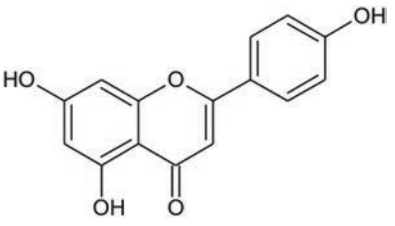

Figure 1. Chemical structure of apigenin.

with PEGylated and folate-receptor targeted PLGA-based NPs with the intention of enhancing the therapeutic potential of apigenin in breast cancer.

EXPERIMENTAL DETAILS

Materials

The following materials were sourced for this study: PLGA (Polylactide-co-glycolide) with a composition of 50/50 and a molecular weight of 43,900 was procured from Durect Corporation, located in Birmingham, AL. N,N-dicyclohexylcarbodiimide (DCC), apigenin, and triethylamine (TEA) were obtained from Alfa Aesar in Heysham, Lancashire, UK. N-hydroxysuccinimide (NHS) was acquired from FlukaChemie, GmbH, based in Germany. Folic acid (FA), Tween-80, and 3-(4,5-dimethylthiazol-2-yl)-3,5-diphenyl tetrazolium bromide (MTT) were purchased from Sigma–Aldrich, situated in St. Louis, MO. Mannitol was sourced from Spectrum Pharmaceuticals in New Brunswick, NJ, and sucrose and coumarin-6 were obtained from MP Biomedical, headquartered in Solon, OH.

For cell culture experiments, we obtained DMEM, trypsin, DMSO, and PBS from Mediatech Inc. in Manassas, VA, USA. Polyether diamine featuring a predominant polyethylene glycol (PEG) backbone (Jeffamine ED-2003 XTJ-502, MW 2000) was kindly provided as a gift by Huntsman International LLC in Austin, TX, and is referred to as PEG-bis-amine in this article. Kolliphor P 407 (P407) was received as a gift from BASF Corporation in Florham Park, NJ. All other solvents and reagents utilized in the study met analytical grade standards. Ultrapure water from the Millipore water purification system in Burlington, MA, was employed in all experimental procedures.

Synthesis of PLGA-PEG and PLGA-PEG-FA Conjugates

PLGA-PEG and PLGA-PEG-FA conjugates were synthesized as reported earlier [10, 20, 21, 40] with some modifications.

Activation of PLGA

PLGA (0.05 mmol), DCC (0.2 mmol), and NHS (0.2 mmol) were dissolved in 10 mL of anhydrous dichloromethane (DCM) in a round-bottom flask (RBF) and stirred in a nitrogen atmosphere at room temperature for 24 h. The byproduct dicyclohexylurea from the resultant mixture was separated by filtering through a syringe filter. Activated PLGA was obtained as filtrate when the filtrate was dropwise added to cold anhydrous diethyl ether. The liquid layer was separated by decantation, and the remaining NHS was removed by repeatedly washing the residual mass with an ice-cold mixture of diethyl ether and methanol (1:1). Finally, activated PLGA was obtained by washing the product with diethyl ether followed by drying under vacuum.

PEGylation of PLGA

To initiate the process, PLGA (0.03 mmol) was solubilized in anhydrous dichloromethane (DCM) in a round-bottom flask (RBF) while continuously stirring. Simultaneously, PEG-bis-amine (0.18 mmol) was similarly dissolved in anhydrous DCM and gradually introduced drop by drop into the PLGA solution. Formation of PLGA-PEG-PLGA triblock copolymers was restricted by addition of excess PEG-bis-amine. The mixture was stirred in the dark under a nitrogen atmosphere for 24 h. The reaction mixture was slowly added to cold methanol to obtain the precipitate, and unreacted PEG-bis-amine was removed from the precipitate by washing with cold methanol. The product was again washed with cold ether, filtered and dried under vacuum to obtain the amine-terminated diblock copolymer (PLGA-PEG-NH_2).

Activation of Folic Acid (Formation of NHS-Folate)

First, folic acid (FA) (0.25 mmol) was activated with DCC (0.5 mmol) and NHS (0.5 mmol) in 10 mL of anhydrous dimethyl sulfoxide (DMSO) in the presence of 0.1 mL triethylamine under a nitrogen atmosphere in the dark overnight. Dicyclohexylurea (the byproduct) was removed by filtration, and then the solution was precipitated in 15 mL of cold anhydrous diethyl ether. The solid was subjected to multiple washes with ether. In order to eliminate DMSO, an excess of acetone was introduced, thoroughly mixed, and set aside. Subsequently, the mixture was gently poured off to collect the resulting product. The product was then thoroughly desiccated under vacuum until complete dryness was achieved.

Conjugation of Folic Acid to PLGA-PEG

Activated FA (0.06 mmol) and PLGA-PEG (0.015 mmol) were co-dissolved in 4 mL anhydrous DMSO in an RBF and allowed to react in the dark under a nitrogen atmosphere at room temperature for 24 h. Maximum conjugation of folic acid to PLGA-PEG was achieved by using excess activated FA. Subsequently, the reaction mixture was introduced into chilled methanol and allowed to stand for 15–20 minutes. Afterward, it was decanted and subjected to vacuum drying. The desiccated material was reconstituted in 15 mL DCM, a step that facilitated the precipitation of free folic acid in DCM while leaving conjugated folic acid in solution. This solution, containing PLGA-PEG-FA, was then passed through a syringe filter, and the resulting filtrate was subjected to vacuum drying.

Determination of Folate Content of the PLGA-PEG-FA Conjugate

To determine the FA content, a specific amount of PEG-PLGA-FA conjugate was dissolved in DMSO and the

absorbance was read at 364 nm. The FA content was determined from the standard curve constructed (concentration vs. absorbance) using different concentrations of FA in DMSO [21, 41].

Chemical Characterization of PLGA-PEG and PLGA-PEG-FA Conjugates

The characterization of the synthesized PLGA-PEG and PLGA-PEG-FA conjugates was conducted through proton nuclear magnetic resonance (^{1}H NMR) analysis. This analysis was performed using a Bruker 400 MHz NMR spectrometer situated in Billerica, MA, with dimethyl sulfoxide-d6 serving as the solvent.

Preparation of Nanoparticles

Nanoparticles (NPs) were fabricated utilizing the nanoprecipitation method as previously documented [10, 42]. In summary, a mixture comprising the polymer (PLGA, or PLGA-PEG, or PLGA-PEG-FA, 13.5 mg) and the drug, apigenin (1.5 mg), was dissolved in 2.5 mL of acetone. This organic solution was introduced gradually into a 10 mL aqueous P407 solution (0.5% w/v) and agitated at 500 rpm using a magnetic stirrer for 4 h. During this period, the organic solvent was evaporated, and the NP suspension was centrifuged at 25,000 g for 45 min at 4°C. The NP pellet formed was suspended in 3.0 mL of deionized (DI) water, kept at −80 °C for 2 h and then freeze dried overnight (FreeZone® Plus™, Labconco Corporation, MO, USA). All batches were prepared in triplicate. Blank NPs were prepared by adding polymer into acetone without the drug.

Characterization of Nanoparticles

Particle Size and Zeta Potential

To assess the particle size, polydispersity index, and zeta potential of the prepared nanoparticles, a Particle Size and Zeta Potential Analyzer (NanoBrook 90 Plus PALS, Brookhaven Instruments, Holtsville, NY) was employed. All measurements were performed in triplicate.

Drug Loading and Encapsulation Efficiency

Accurately weighed, 1.0 mg of NPs was dissolved in a solvent mixture of DCM and ethanol (3:7) by sonication and filtered through a 0.22 μ PVDF membrane filter (Millex®-GV Syringe driven filter unit, Millipore Corporation, Bedford, MA, USA). The absorbance was determined using UV-spectrophotometry (Varioskan Flash, Thermo Scientific, USA) at a wavelength of 337 nm. A blank nanoparticle solution, prepared in a similar manner, was employed as a blank. The percentage of encapsulation efficiency (% EE) and drug loading (% DL) were computed using the subsequent formula.

$$\%\ \text{EE} = \text{amount of apigenin loaded in the NPs (mg)} / \text{amount of apigenin used for preparation of NPs (mg)} \times 100$$

$$\%\ \text{DL} = \text{amount of apigenin loaded in the prepared NPs (mg)} / \text{amount of apigenin and polymer used for preparation of NPs (mg)} \times 100$$

In Vitro Drug Release Study

NP suspension of different PLGA based NPs containing 175 μg of apigenin was taken in a dialysis bag (Spectra/Por molecular porous membrane, MWCO 6–8000, Spectrum Laboratories Inc., CA, USA) and tied with threads on both sides. The dialysis bag was immersed in an amber glass vial containing 35 mL of PBS, pH 7.4, with 0.5% Tween 80. The vial was placed in an horizontal shaking incubator at 37 °C and 100 rpm. For determining release of apigenin from different PLGA based formulations, one mL of medium was withdrawn from each vial and substituted with fresh media. Apigenin concentration in the withdrawn media was determined by UV-spectrophotometry and represented as cumulative drug release using the following formula. The experiments were performed in triplicate.

$$\%\ \text{Drug Release} = \text{amount of apigenin released in the medium } (\mu\text{g}) / \text{amount of apigenin loaded in the NPs } (\mu\text{g}) \times 100$$

Effect of Cryoprotectants on the Particle Size of Nanoparticles After Lyophilization

The role of cryoprotectants such as sucrose and mannitol were analyzed on the size growth of the NPs due to lyophilization. Briefly, NP suspension and equal volume of mannitol or sucrose solution was taken in amber vials separately. The concentration of mannitol or sucrose in the final mixture was 10% and 5%, respectively. These vials were kept in a deep freezer (−80 °C) for 2 h followed by lyophilization overnight. The particle size of these freeze dried NPs was determined by the DLS method and compared with the particle size of lyophilized NPs prepared without addition of cryoprotectants.

Cell Lines and Culture

The MCF-7 breast cancer cell line was procured from ATCC (Manassas, VA). These cells were cultivated in T75 flasks, with Dulbecco's modified Eagle's medium (DMEM) supplemented with 10% fetal bovine serum (obtained from Mediatech, Manassas, VA), and 1% penicillin/streptomycin (Penicillin Streptomycin Solution 100X, comprising 10,000 IU/mL penicillin and 10,000 μg/mL streptomycin, also obtained from Mediatech, Manassas, VA). The cells were maintained in a

humidified atmosphere at 37 °C with 5% carbon dioxide. Passaging of cells was carried out upon reaching confluence, following trypsinization.

In Vitro Cytotoxicity Study

MCF-7 cells were seeded into 96 well tissue culture plates at a density of 3000 cells/well. Following a 24-h incubation period, the existing culture medium was replaced with a fresh medium, which contained either the pure drug or drug-loaded nanoparticles (NPs) at varying concentrations ranging from 6.25 to 100 μM. To a set of wells only fresh medium was added without any drug (negative control). The plates were incubated for 72 h and then the media was removed and cells were washed with PBS. To each well, 50 μl of MTT solution (0.5 mg/ml) in media was added and further incubated for 4 h under similar conditions. MTT reacted with the mitochondrial enzyme of live cells to form the formazan crystals and the crystals were dissolved by adding 100 μl of DMSO into each well. Cell viability was determined by quantifying the absorbance of the transformed dye at a wavelength of 570 nm using a microplate reader.

$$\%\ \text{cell viability} = \text{Absorbance of treatment}/\text{Absorbance of control} \times 100$$

Statistical Analysis

Data are represented as the mean ± standard error of the mean (SEM), except in the case of drug loading, encapsulation efficiency, particle size, and zeta potential, where the data are the mean ± standard deviation (SD). The *in vitro* cytotoxicity data were statistically analyzed for significance by two-way analysis of variance (ANOVA) followed by Bonferroni post hoc tests using GraphPad Prism 7.0 software (GraphPad Software, La Jolla, CA). $P < 0.05$ was considered statistically significant.

RESULTS AND DISCUSSION

Preparation and Characterization of PLGA-PEG and PLGA-PEG-FA Conjugates

The conjugates were synthesized as depicted in the following scheme (Fig. 2).

The synthesis of these conjugates entails the establishment of amide bonds. To initiate the formation of these bonds, a succinimide end group (PLGA-NHS) is initially generated from a carboxylic group (PLGA-COOH). This PLGA-NHS group is then coupled with an amine group (NH_2). Following the conjugation of folic acid (FA) to the polymer, the conversion of the COOH group of FA into the more reactive NHS group facilitates the creation of the succinimide derivative. This derivative subsequently reacts with the free primary NH_2 group of the PLGA-PEG copolymer. It's worth noting that, during the preparation of NPs, the FA moiety is oriented outward [10, 21]. The successful conjugation of FA to PLGA-PEG was verified through ^{1}H NMR analysis, and the various assigned peaks are detailed in Table I. Furthermore, the percentage of FA conjugated to PLGA-PEG was found to be 43.2% based on the molar ratio.

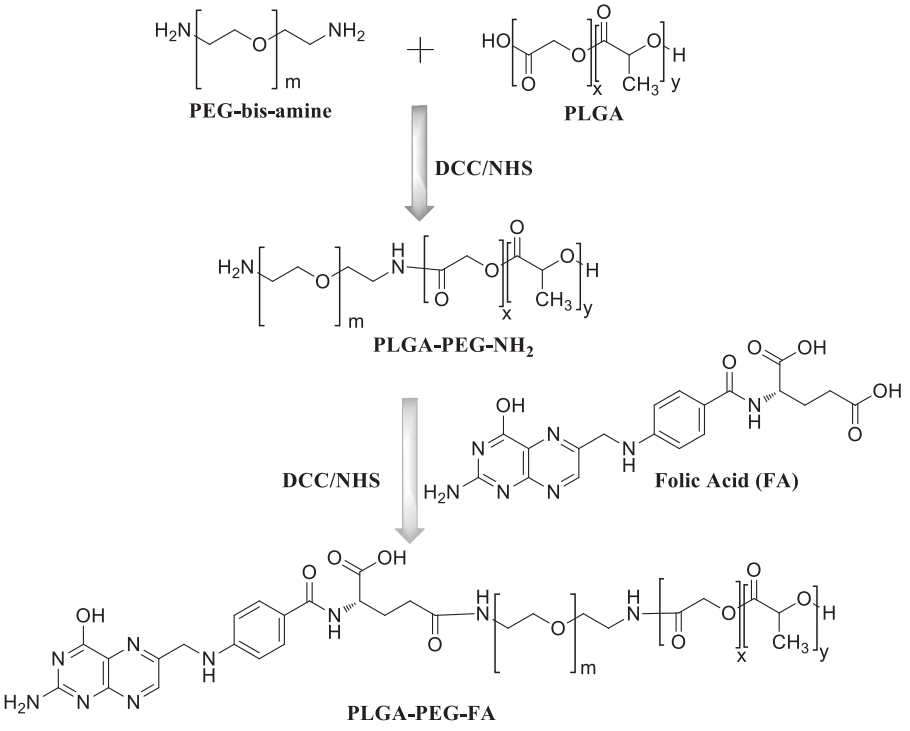

Figure 2. **Synthetic scheme of PLGA-PEG and PLGA-PEG-FA conjugates.**

Table I. **^{1}H NMR (DMSO-d_6) peaks of PLGA-PEG and PLGA-PEG-FA conjugates.**

Polymer	$\delta_{(ppm)}$	Assignment
PLGA-PEG	1.5	(3H, $-CH_3$ of poly(glycolide))
	4.8–5.3	(H, poly(D,L-lactide) and poly(glycolide))
	3.6	(H, PEG-bis-amine)
	7.3	(2H, NH_2 of PEG-bis-amine)
PLGA-PEG-FA	6.4–6.7	(COOH, folate)
	6.9	(H, aromatic ring)
	7.6	(m,4H, aromatic ring)
	8.0–8.2	(NH, folate)
	8.6	(NH_2, folate)
	11.35	(OH, folate)

Preparation and Characterization of Apigenin-Loaded PLGA-Based Nanoparticles

NPs of PLGA, PLGA-PEG, and PLGA-PEG-FA were produced via the nano-precipitation method. These NPs underwent characterization, including assessment of particle size, polydispersity index (PDI), and zeta potential using dynamic light scattering (DLS). Encapsulation efficiency was quantified using UV-Visible spectroscopy.

Through a series of preliminary experiments involving the testing of various stabilizers (PVA or P407), diverse drug and polymer concentrations, and different ratios of acetone to water, it was established that the optimal conditions for PLGA NP preparation included a P407 concentration of 0.5% (w/v), a drug and polymer ratio of 1:9 (w/w), and a 1:4 ratio of the organic phase to the aqueous phase (v/v). These same conditions were applied for the preparation of PLGA-PEG and PLGA-PEG-FA NPs.

The physicochemical parameters of various PLGA based NPs are presented in Table II. The particle size of the PLGA-PEG and PLGA-PEG-FA NPs were smaller than that of the PLGA NPs (Fig. 3). The decrease in the particle size may be due to the presence of hydrophilic PEG groups on the surface of the NPs, which increases the stability of the NPs. Similar findings have been reported previously [21, 43]. NPs with particle size <200 nm are not prone to phagocytic uptake and remain in the circulation system for a longer period. Hence for better effectiveness of the nano-formulations, one of the most important criteria of the nano-carrier system is to achieve the desired particle size of 100–200 nm [25, 44]. Polydispersity index, PDI, is measured to illustrate the heterogenisity of particle size distribution. PDI of ≥ 0.7 are not suitable for analysis as size distribution is high and a value of ≤ 0.05 are highly monodisperse. The desired PDI value for polymer-based NPs is ≤ 0.2 [45]. In the present study, the PDI values of FA-targeted PLGA-based NPs are <0.2 indicating the stability and acceptability of the formulations. The surface charge of the NPs is negative. The zeta potential of PLGA-PEG-FA NPs is lower than that of PLGA and PLGA-PEG NPs (Fig. 4), which may be attributed to the protonated amino acid group in FA, which helps further reduce the negative charge [20, 21]. The moderate zeta potential values may provide stability of the NPs, and the negative charges on the surface of the NP indicate their non-genotoxic and non-cytotoxic nature [46]. Positively charged NPs may be toxic to normal cells as the anionic surface charge of normal cells would help in enhanced cellular uptake. However, negative zeta potential of NPs is suitable for carrier systems as it prevents macrophage opsonization and plasma protein aggregation [47]. The drug loading (DL, % w/w) and encapsulation efficiency (EE, % w/w) were reasonably good. The DL and EE of both PLGA-PEG and PLGA-PEG-FA NPs exhibited slightly higher compared to PLGA NPs.

The PLGA-based NPs were not analyzed for surface morphology by scanning electron microscopy or transmission electron microscopy, but previous studies suggest that similar NPs have spherical shape and smooth surface [25, 48, 49].

In Vitro Release of Apigenin

The dialysis bag method was adopted to analyze the *in vitro* release of apigenin from different nano formulations in PBS (pH 7.4) containing 0.5% Tween 80 at 37 °C. Apigenin in DMSO solution was almost completely released from the dialysis bag within 8 h (Fig. 5). The release of apigenin from apigenin-loaded PLGA NPs and apigenin-loaded PLGA-PEG NPs was similar, with 18 and 17% cumulative drug release after 8 h, respectively, whereas apigenin-loaded PLGA-PEG-FA NPs exhibited slower release of apigenin, with around 9% drug release after 8 h. The release of apigenin was sustained for up to 7 days. Apigenin was released (approximately 82%) from the apigenin-loaded PLGA NPs after 7 days. However, the release of apigenin from the apigenin-loaded PLGA-PEG and PLGA-PEG-FA NPs after 7 days was approximately 93% which is relatively higher than that of the PLGA NPs. The slightly higher release of apigenin from PLGA-PEG

Table II. **Physicochemical characteristics of different polymeric NPs containing apigenin.**

Formulation	Particle size (nm)	Polydispersity index	Zeta potential (mV)	Drug loading (% w/w)	Encapsulation Efficiency (% w/w)
PLGA NPs	187.35 ± 3.54	0.282 ± 0.016	-25.58 ± 2.68	7.88 ± 0.63	78.80 ± 6.31
PLGA-PEG NPs	142.78 ± 2.31	0.182 ± 0.017	-24.45 ± 1.22	8.25 ± 0.33	82.51 ± 3.29
PLGA-PEG-FA NPs	177.97 ± 2.84	0.178 ± 0.013	-29.52 ± 2.12	8.02 ± 0.42	80.20 ± 4.19

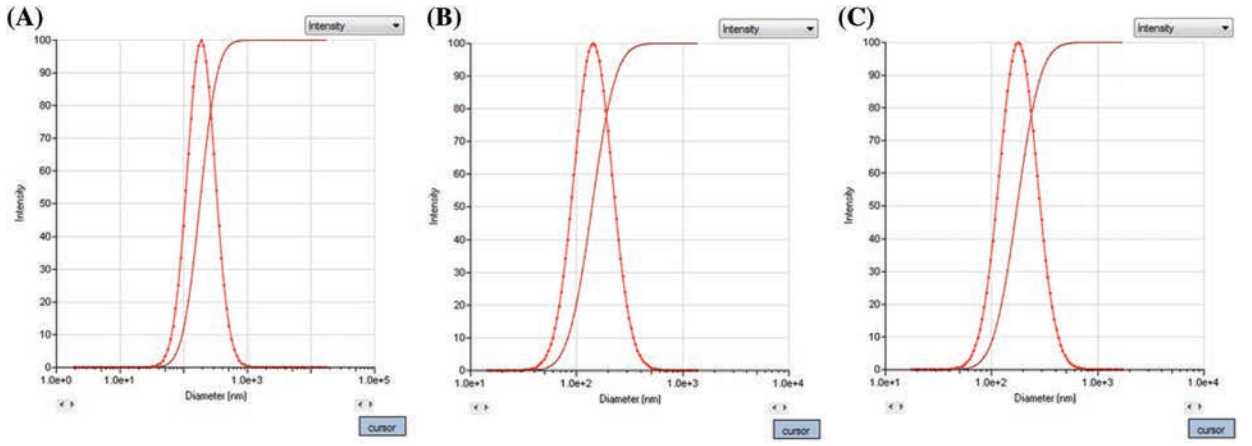

Figure 3. **Particle size of PLGA (A), PLGA-PEG (B) and PLGA-PEG-FA (C) NPs loaded with apigenin after lyophilization.**

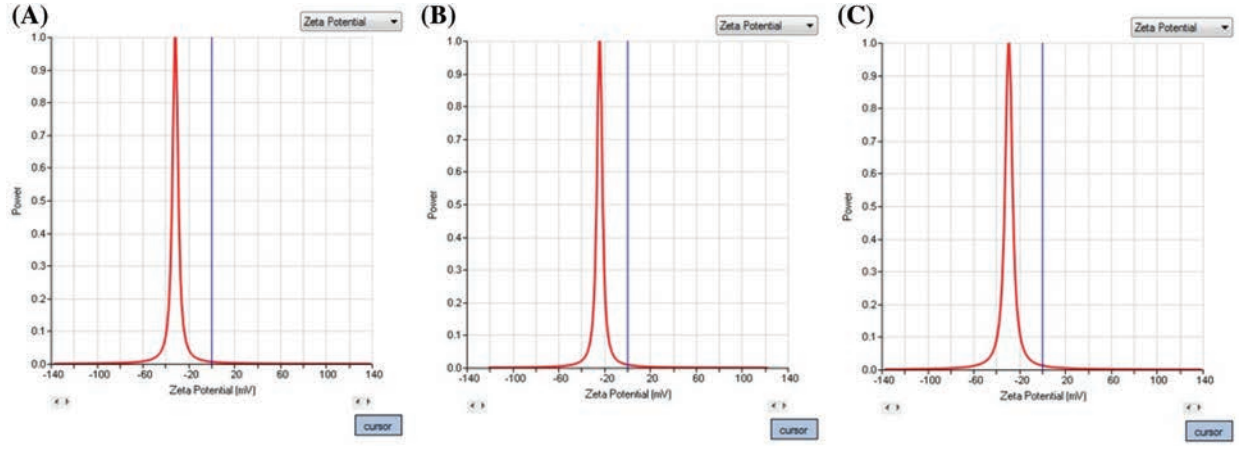

Figure 4. **Zeta potential of PLGA (A), PLGA-PEG (B) and PLGA-PEG-FA (C) NPs loaded with apigenin after lyophilization.**

and PLGA-PEG-FA NPs compared to PLGA NPs may be due to the smaller particle size and presence of the PEG moiety, which provides a greater hydrophilic surface. NPs with a hydrophilic surface absorb more water from the aqueous medium because of enhanced interaction, which cause enhanced polymer degradation and drug release from the polymer matrix. The slow release of apigenin from the polymeric NPs may be due to the presence of the drug in the core of the NP structure, which required breakdown of the polymer for drug release. The various mechanisms of drug release are diffusion of the drug, erosion and swelling of the polymer matrix and break down of polymer. The polymer, PLGA, degraded slowly; hence, the release of the drug from the NPs predominantly relied on drug diffusion and matrix erosion.

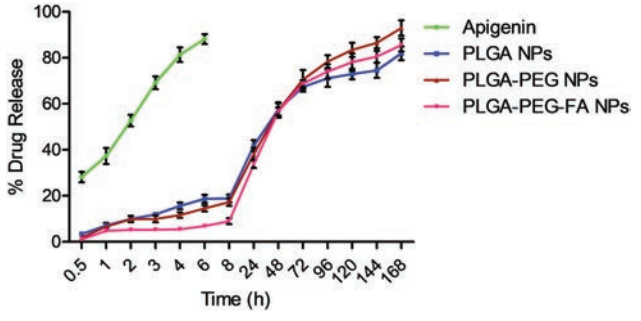

Figure 5. ***In vitro*** **release profiles of apigenin from PLGA-based NP in PBS (pH 7.4) at 37 °C. Data are presented as the mean ± standard error of the mean (SEM), (*n* = 3).**

Furthermore, the release kinetics was also studied for all three PLGA-based NPs: zero-order kinetic model (% cumulative drug release vs. time), first-order kinetic model (log % cumulative drug release vs. time), Higuchi model (% cumulative drug release vs. square root of time) and Korsmeyer–Peppas model (log % cumulative drug release vs. log time). Notably, the highest correlation (R^2) values, which serve as indicators of the best fit, were observed for PLGA, PLGA-PEG, and PLGA-PEG-FA NPs containing apigenin, with values of 0.969, 0.989, and 0.987, respectively (Figs. 6–8). These values confirm that PLGA and PLGA-PEG NPs followed the Higuchi model, whereas PLGA-PEG-FA NPs followed the zero-order kinetic model.

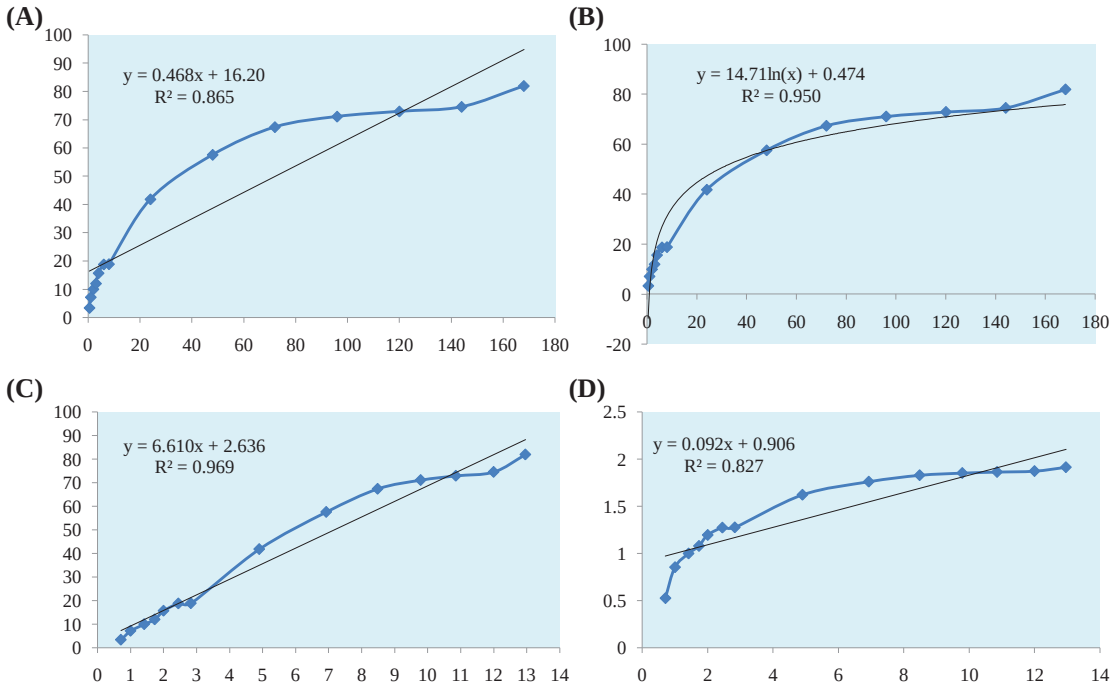

Figure 6. **Drug release kinetics plots for PLGA NPs containing apigenin: Zero-order plot (A), first-order plot (B), Higuchi plot (C) and Korsmeyer Peppas plot (D).**

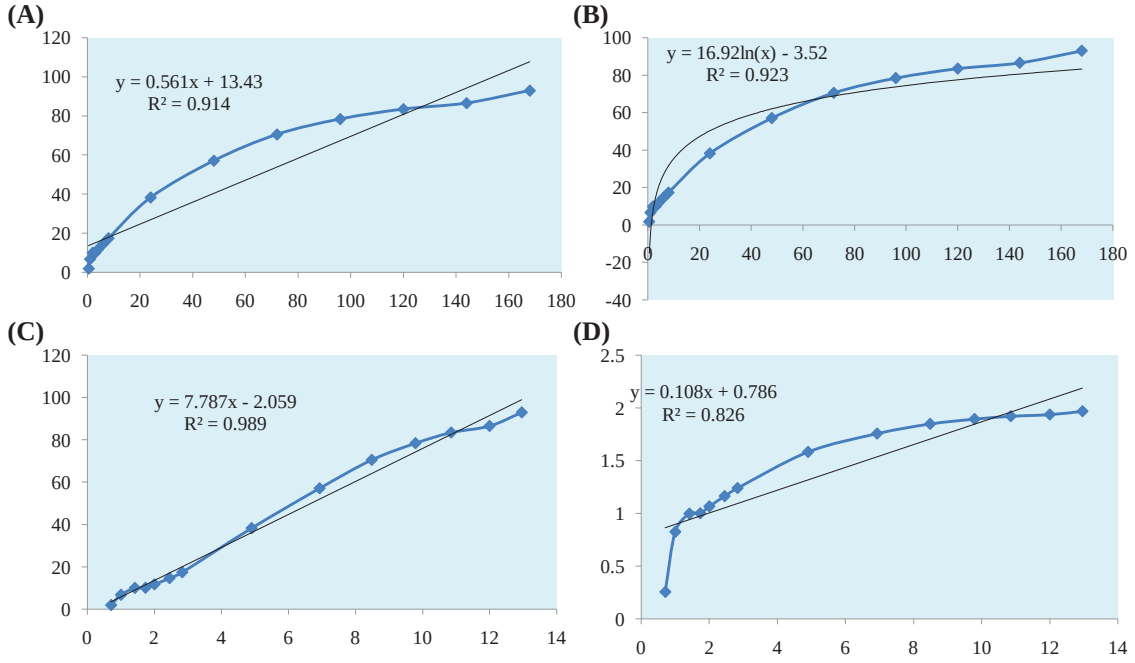

Figure 7. **Drug release kinetics plots for PLGA-PEG NPs containing apigenin: Zero-order plot (A), first-order plot (B), Higuchi plot (C) and Korsmeyer Peppas plot (D).**

Effect of Cryoprotectants on the Particle Size of Nanoparticles After Lyophilization

Lyophilization of the NPs increase in the particle size as alteration of physical state and stress due to freeze-drying causes aggregation of NPs. In a prior study, we documented that the introduction of sucrose (5%) and mannitol (10%) into the NP suspension prior to lyophilization effectively mitigated the enlargement of NP size. Cryoprotectants, typically sugars, establish hydrogen bonds with the NPs, thus shielding them from aggregation and

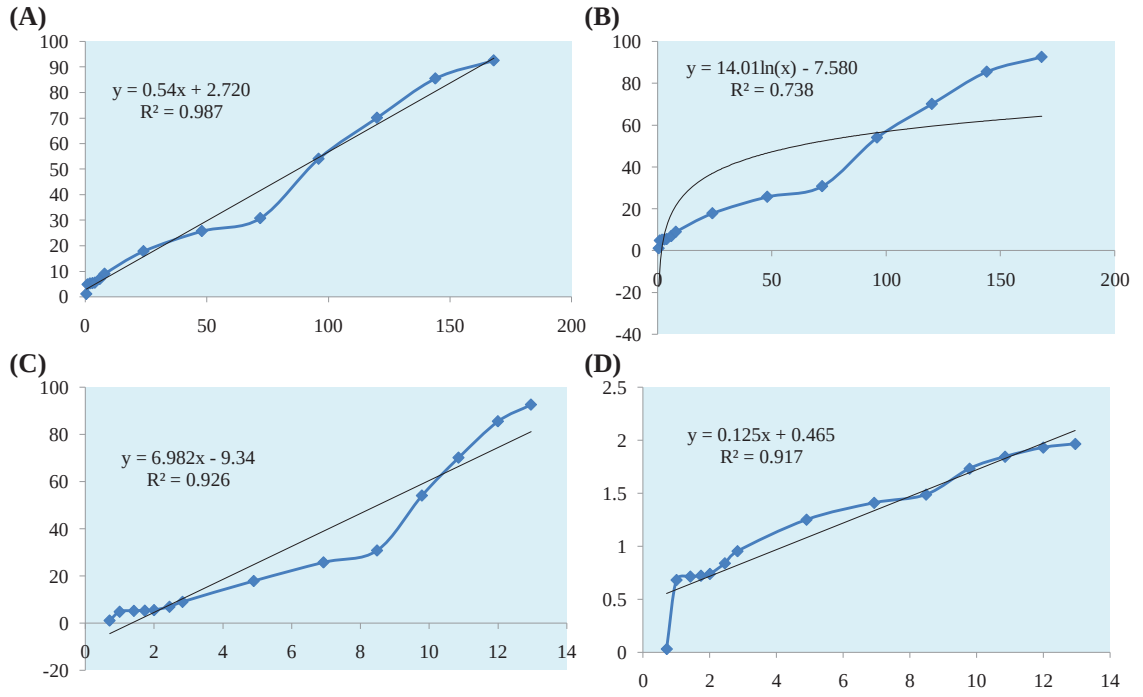

Figure 8. **Drug release kinetics plots for PLGA-PEG-FA NPs containing apigenin: Zero-order plot (A), first-order plot (B), Higuchi plot (C) and Korsmeyer Peppas plot (D).**

the stresses associated with freezing. In the present investigation, both sugars were found to curtail the rise in particle size induced by the freeze-drying process, as depicted in Figure 9. It is worth noting that mannitol (10%) demonstrated superior efficacy in controlling the particle size of the NPs when compared to sucrose (5%) [10, 22]. The % reduction was minimal, approximately 10% with sucrose and 16% with mannitol. Lyophilized NPs without cryoprotectants were used for physicochemical characterization and biological evaluation.

In Vitro Cytotoxicity Study

Figure 10 represents the *in vitro* anticancer potential of different concentrations of pure apigenin and various PLGA based nano-formulations containing apigenin in a breast cancer cell line (MCF-7) by MTT assay. PLGA-based NPs produced a better effect than the pristine drug and the order of anticancer activity of different NPs was PLGA-PEG-FA > PLGA-PEG > PLGA (Fig. 11). PLGA NPs containing apigenin exhibited significantly higher cytotoxicity than pure apigenin only at the highest tested concentration (100 μM), whereas PLGA-PEG and PLGA-PEG-FA NPs containing apigenin showed significantly enhanced anticancer effects at all the tested doses compared to free drug. The half maximal inhibitory concentration (IC_{50}) values of apigenin, apigenin-loaded

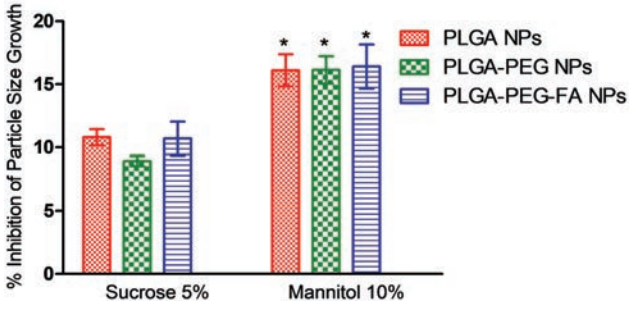

Figure 9. **Effect of cryoprotectant on particle size after freeze-drying (mean ± SEM, $n = 3$); *, $P < 0.05$ vs. sucrose 5%.**

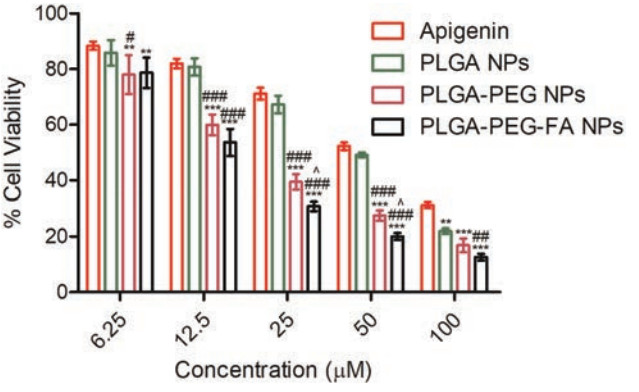

Figure 10. ***In vitro*** **cytotoxicity of apigenin and apigenin-loaded PLGA, PLGA-PEG and PLGA-PEG-FA NPs against a breast cancer cell line (MCF-7) after 72 hours of incubation (mean ± SEM, $n = 3$). $^{**}P < 0.01$, $^{***}P < 0.001$ versus apigenin treatment at the same dose; $^{\#}P < 0.05$, $^{\#\#}P < 0.01$, $^{\#\#\#}P < 0.001$ versus PLGA NPs containing apigenin treatment at the same dose; $^{\wedge}P < 0.05$ versus PLGA-PEG NPs containing apigenin treatment at the same dose.**

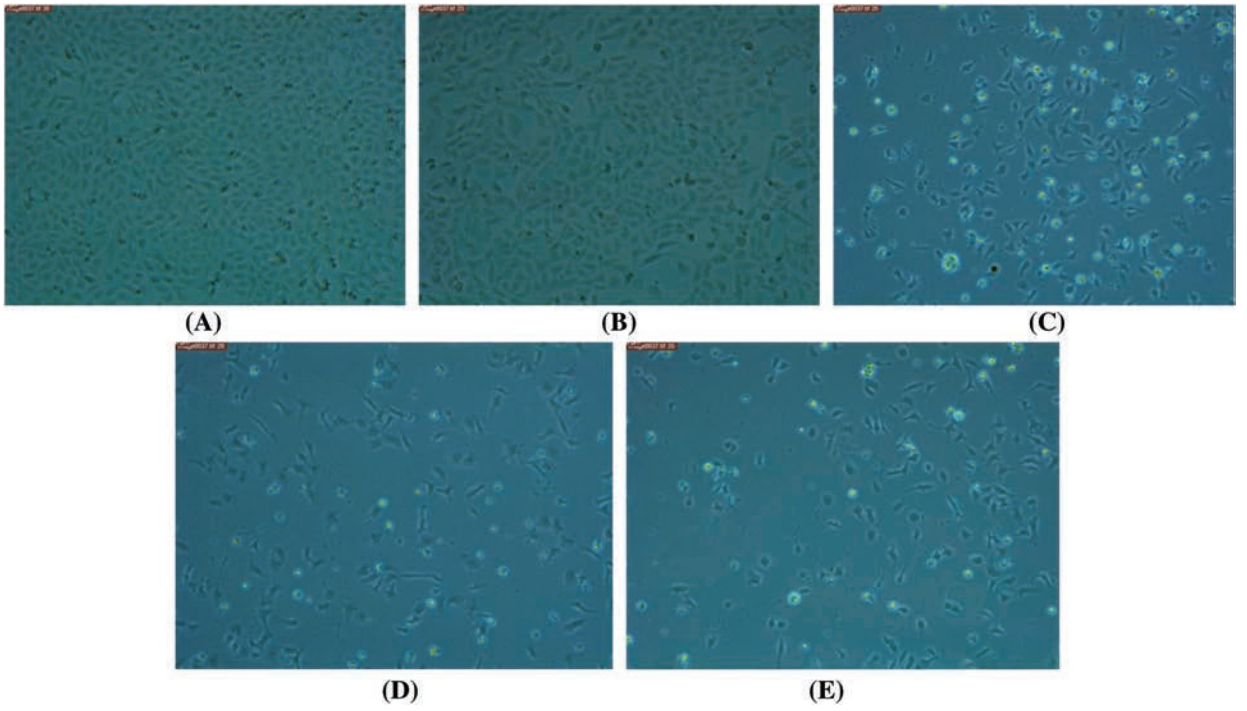

Figure 11. ***In vitro*** **cytotoxicity study of different treatments. Cells treated with only media, negative control (A), cells treated with pure APG (B), cells treated with PLGA-APG NPs (C), cells treated with PLGA-PEG-APG NPs (D), and cells treated with PLGA-PEG-FA-APG NPs (E). Images were captured by a phase contrast microscope (Leica, Germany) with magnification of 200x.**

PLGA, PLGA-PEG and PLGA-PEG-FA NPs were 50.2, 49.4, 18.1 and 13.3 μM, respectively. Apigenin-loaded PLGA-PEG and PLGA-PEG-FA NPs showed 2.79- and 3.77-fold increased cytotoxicity than uncapsulated apigenin. The cytotoxicity of PLGA-PEG-FA NPs containing apigenin was significantly higher ($P < 0.05$) than that of PLGA-PEG NPs containing apigenin at higher tested concentrations. The enhanced cytotoxicity of the PEGylated and folate receptor-targeted NPs loaded with apigenin compared to pure apigenin may be due to their small size, which facilitates enhanced cell permeability. Also, the NPs may not be subjected to p-glycoprotein efflux like pure drugs. The PLGA-PEG-FA NPs showed enhanced anticancer effects as the NPs can enhance cellular internalization via folate receptor-mediated endocytosis and circumvent the efflux of apigenin by P-gp pumps. Increased cellular uptake of folate receptor-targeted NPs was reported in our earlier study and some other reports [10, 40, 50]. These effects increased the anticancer effect of apigenin-loaded PLGA-PEG-FA NPs in folate receptor overexpressing breast cancer cells, MCF-7. Empty NPs (without the drug molecule, apigenin) showed negligible cytotoxicity (Fig. 12).

Folate receptor-targeted nanocarriers have been successfully used for the targeted delivery of anticancer molecules in different cancer cells overexpressing the folate receptor. The anticancer activity of folate receptor-targeted NPs encapsulated with doxorubicin exhibited enhanced anticancer activity (*in vitro* and *in vivo*). Furthermore, no

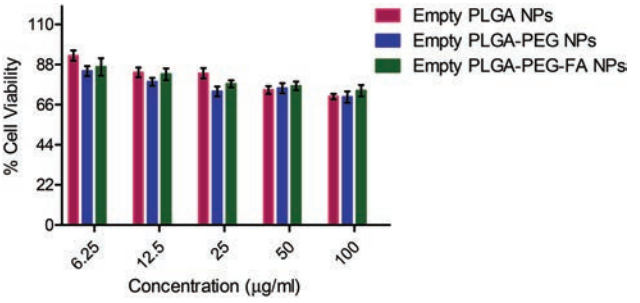

Figure 12. ***In vitro*** **cytotoxicity of empty (without apigenin) PLGA, PLGA-PEG and PLGA-PEG-FA NPs against a breast cancer cell line (MCF-7) after 72 hours of incubation (mean ± SEM, $n = 3$).**

significant toxicity in the liver, lung, kidney, and heart of nude mice with xenograft MCF-7 breast tumors was observed after 35 days of treatment [51]. Folic acid-conjugated cyclodextrin NPs containing paclitaxel are non-toxic and produce increased anticancer effects in metastatic breast cancer [52]. It could be postulated that folate receptor-targeted formulations increase the anticancer effect and decrease the side effects of the drug candidate because of enhanced cellular internalization, resulting in less drug requirement to produce the effect. In the present study, folate receptor-targeted NPs containing apigenin were small in size, showed sustained drug release behavior and exhibited enhanced *in vitro* cytotoxicity in folate receptor overexpressing MCF-7 breast cancer cells.

CONCLUSIONS

In the present study, folate-decorated PLGA NPs containing apigenin were fabricated by nanoprecipitation method. The NPs were small in size with high encapsulation efficiency, showed sustained release of the drug and produced pronounced anticancer effects in folate receptor overexpressing breast cancer cells (MCF-7). PLGA-PEG-FA NPs may be a promising approach for targeted delivery of apigenin in breast cancer. Further studies are needed to explore the *in vivo* efficacy of the prepared NPs. Also, the PLGA-PEG-FA NPs could be explored for co-delivery of drugs and theranostic purposes, and in other folate receptor overexpressing cancers.

Declaration of Interest

The authors declare no conflict of interest.

Acknowledgment: This work was supported by the University Grants Commission, New Delhi, India (F.NO.5-63/2016[IC]) as Raman Fellowship for Postdoctoral Research in the USA to AP. The authors are thankful to California State University, Fresno, CA for NMR analyses. The authors would like to extend their sincere appreciation to the Researchers Supporting Project Number (RSP2023R301), King Saud University, Riyadh, Saudi Arabia.

REFERENCES

1. Verma, L.T., Singh, N., Gorain, B., Choudhury, H., Tambuwala, M.M., Kesharwani, P. and Shukla, R., **2020**. Recent advances in self-assembled nanoparticles for drug delivery. *Current Drug Delivery*, *17*(4), pp.279–291.
2. de Rinaldis, E., Tutt, A. and Dontu, G., **2016**. Breast cancer facts and figures. *Breast Pathology*, *47*, pp.352–359.
3. Ayub, A.D., Chiu, H.I., Mat Yusuf, S.N.A., Abd Kadir, E., Ngalim, S.H. and Lim, V., **2019**. Biocompatible disulphide cross-linked sodium alginate derivative nanoparticles for oral colon-targeted drug delivery. *Artificial Cells, Nanomedicine and Biotechnology*, *47*(1), pp.353–369.
4. Chiu, H.I., Samad, N.A., Fang, L. and Lim, V., **2021**. Cytotoxicity of targeted PLGA nanoparticles: A systematic review. *RSC Advances*, *11*, pp.9433–9449.
5. Schoubben, A., Ricci, M. and Giovagnoli, S., **2019**. Meeting the unmet: From traditional to cutting-edge techniques for poly lactide and poly lactide-co-glycolide microparticle manufacturing. *Journal of Pharmaceutical Investigation*, *49*, pp.381–404.
6. Kim, K.T., Lee, J.Y., Kim, D.D., Yoon, I.S. and Cho, H.J., **2019**. Recent progress in the development of poly(lactic-co-glycolic acid)-based nanostructures for cancer imaging and therapy. *Pharmaceutics*, *11*(6), p.280.
7. Yoo, J., Park, C., Yi, G., Lee, D. and Koo, H., **2019**. Active targeting strategies using biological ligands for nanoparticle drug delivery systems. *Cancers*, *11*(5), p.640.
8. Bertrand, N., Wu, J., Xu, X., Kamaly, N. and Farokhzad, O.C., **2014**. Cancer nanotechnology: The impact of passive and active targeting in the era of modern cancer biology. *Advanced Drug Delivery Reviews*, *66*, pp.2–25.
9. Zhong, S., Zhang, H., Liu, Y., Wang, G., Shi, C., Li, Z., Feng, Y. and Cui, X., **2017**. Folic acid functionalized reduction-responsive magnetic chitosan nanocapsules for targeted delivery and triggered release of drugs. *Carbohydrate Polymer*, 168, pp.282–289.
10. Saxena, V., Naguib, Y. and Hussain, M.D., **2012**. Folate receptor targeted 17-allylamino-17-demethoxygeldanamycin (17-AAG) loaded polymeric nanoparticles for breast cancer. *Colloids and Surfaces B: Biointerfaces*, *94*, pp.274–280.
11. Dhas, N.L., Ige, P.P. and Kudarha, R.R., **2015**. Design, optimization and in-vitro study of folic acid conjugated-chitosan functionalized PLGA nanoparticle for delivery of bicalutamide in prostate cancer. *Powder Technology*, *283*, pp.234–245.
12. Tagde, P., Kulkarni, G.T., Mishra, D.K. and Kesharwani, P., **2020**. Recent advances in folic acid engineered nanocarriers for treatment of breast cancer. *Journal of Drug Delivery Science and Technology*, *56*, p.101613.
13. Narmani, A., Mohammadnejad, J. and Yavari, K., **2019**. Synthesis and evaluation of polyethylene glycol- and folic acid-conjugated polyamidoamine G4 dendrimer as nanocarrier. *Journal of Drug Delivery Sciences and Technology*, *50*, pp.278–286.
14. Young, O., Ngo, N., Lin, L., Stanbery, L., Creeden, J.F., Hamouda, D. and Nemunaitis, J., **2023**. Folate receptor as a biomarker and therapeutic target in solid tumors. *Current Problems in Cancer*, *47*, p.100917.
15. Varaganti, P., Buddolla, V., Lakshmi, B.A. and Young-Joon Kim, Y.J., **2023**. Recent advances in using folate receptor 1 (FOLR1) for cancer diagnosis and treatment, with an emphasis on cancers that affect women. *Life Science*, *326*, p.121802.
16. Gupta, A., Kaur, C.D., Saraf, S. and Saraf, S., **2017**. Targeting of herbal bioactives through folate receptors: A novel concept to enhance intracellular drug delivery in cancer therapy. *Journal of Receptors and Signal Transduction*, *37*(3), pp.314–323.
17. Granja, A., Nunes, C., Sousa, C.T. and Reis, S., **2022**. Folate receptor-mediated delivery of mitoxantrone-loaded solid lipid nanoparticles to breast cancer cells. *Biomedicine & Pharmacotherapy*, *154*, p.113525.
18. Ahmed, S.A., Parama, D., Daimari, E., Girisa, S., Banik, K., Harsha, C., Dutta, U. and Kunnumakkara, A.B., **2021**. Rationalizing the therapeutic potential of apigenin against cancer. *Life Sciences*, *267*, p.118814.
19. Shanmugam, M.K., Warrier, S., Kumar, A.P., Sethi, G. and Arfuso, F., **2017**. Potential role of natural compounds as anti-angiogenic agents in cancer. *Current Vascular Pharmacology*, *15*(6), pp.503–519.
20. Liang, C., Yang, Y., Ling, Y., Huang, Y., Li, T. and Li, X., **2011**. Improved therapeutic effect of folate-decorated PLGA-PEG nanoparticles for endometrial carcinoma. *Bioorganic Meicinal Chemistry*, *19*(13), pp.4057–4066.
21. El-Hammadi, M.M., Delgado, A.V., Melguizo, C., Prados, J.C. and Arias, J.L., **2017**. Folic acid-decorated and PEGylated PLGA nanoparticles for improving the antitumour activity of 5-fluorouracil. *International Journal of Pharmaceutics*, *516*(1–2), pp.61–70.
22. Patra, A., Satpathy, S., Naik, P.K., Kazi, M. and Hussain, M.D., **2022**. Folate receptor-targeted PLGA-PEG nanoparticles for enhancing the activity of genistein in ovarian cancer. *Artificial Cells, Nanomedicine and Biotechnology*, *50*(1), pp.228–239.
23. Wei, K., Peng, X. and Zou, F., **2014**. Folate-decorated PEG-PLGA nanoparticles with silica shells for capecitabine controlled and targeted delivery. *International Journal of Pharmaceutics*, *464*(1–2), pp.225–233.
24. Chen, J., Li, S. and Shen, Q., **2012**. Folic acid and cell-penetrating peptide conjugated PLGA–PEG bifunctional nanoparticles for vincristine sulphate delivery. *European Journal of Pharmaceutical Sciences*, *47*(2), pp.430–443.
25. Akbarian, A., Ebtekara, M., Pakravan, N. and Hassan, Z.M., **2020**. Folate receptor alpha targeted delivery of artemether to breast cancer cells with folate-decorated human serum albumin nanoparticles. *International Journal of Biological Macromolecules*, *152*, pp.90–101.

26. Yan, X., Qi, M., Li, P., Zhan, Y. and Shao, H., **2017**. Apigenin in cancer therapy: Anti-cancer effects and mechanisms of action. *Cell and Bioscience*, *7*, p.50.

27. Madunic, I.V., Madunic, J., Antunovic, M., Paradzik, M., Garaj-Vrhovac, V., Breljak, D., Marijanovic, I. and Gajski, G., **2018**. Apigenin, a dietary flavonoid, induces apoptosis, DNA damage, and oxidative stress in human breast cancer MCF-7 and MDA MB-231 cells. *Naunyn-Schmiedeberg's Archives of Pharmacology*, *391*(5), pp.537–550.

28. Nabavi, S.M., Habtemariam, S., Daglia, M. and Nabavi, S.F., **2015**. Apigenin and breast cancers: From chemistry to medicine. *Anti Cancer Agents in Medicinal Chemistry*, *15*(6), pp.728–735.

29. Zhao, G., Han, X., Cheng, W., Ni, J., Zhang, Y., Lin, J. and Song, Z., **2017**. Apigenin inhibits proliferation and invasion, and induces apoptosis and cell cycle arrest in human melanoma cells. *Oncology Reports*, *37*(4), pp.2277–2285.

30. Cao, X., Liu, B., Cao, W., Zhang, W., Zhang, F., Zhao, H., Meng, R., Zhang, L., Niu, R., Hao, X. and Zhang, B., **2013**. Autophagy inhibition enhances apigenin-induced apoptosis in human breast cancer cells. *Chinese Journal of Cancer Research*, *25*(2), pp.212–222.

31. Lee, W.J., Chen, W.K., Wang, C.J., Lin, W.L. and Tseng, T.H., **2008**. Apigenin inhibits HGF-promoted invasive growth and metastasis involving blocking PI3K/Akt pathway and beta 4 integrin function in MDA-MB-231 breast cancer cells. *Toxicology and Applied Pharmacology*, *226*(2), pp.178–191.

32. Li, B., Robinson, D.H. and Birt, D.F., **1997**. Evaluation of properties of apigenin and [G-3H] apigenin and analytic method development. *Journal of Pharmaceutical Sciences*, *86*, pp.721–725.

33. Feng, W.-m., Guo, H.-h., Xue, T., Wang, X., Tang, C.-w., Ying, B., Gong, H. and Cui, G., **2015**. Anti-inflammation and anti-fibrosis with PEGylated, apigenin loaded PLGA nanoparticles in chronic pancreatitis disease. *RSC Advance*, *5*, pp.83628–83635.

34. Wu, W., Zu, Y., Zhao, X., Zhang, X., Wang, L., Li, Y., Wang, L., Zhang, Y. and Lian, B., **2017**. Solubility and dissolution rate improvement of the inclusion complex of apigenin with 2-hydroxypropyl-β-cyclodextrin prepared using the liquid antisolvent precipitation and solvent removal combination methods. *Drug Development and Industrial Pharmacy*, *43*(8), pp.1366–1377.

35. Wojtunik-Kulesza, K., Oniszczuk, A., Oniszczuk, T., Combrzynski, M., Nowakowska, D. and Matwijczuk, A., **2020**. Influence of in vitro digestion on composition, bioaccessibility and antioxidant activity of food polyphenols-a non-systematic review. *Nutrients*, *12*(5), p.1401.

36. Das, S., Das, J., Samadder, A., Paul, A. and Khuda-Bukhsh, A.R., **2013**. Efficacy of PLGA-loaded apigenin nanoparticles in Benzo[a]pyrene and ultraviolet-B induced skin cancer of mice: Mitochondria mediated apoptotic signalling cascades. *Food and Chemical Toxicology*, *62*, pp.670–680.

37. Ganguly, S., Dewanjee, S., Sen, R., Chattopadhyay, D., Ganguly, S., Gaonkar, R. and Debnath, M.C., **2021**. Apigenin-loaded galactose tailored PLGA nanoparticles: A possible strategy for liver targeting to treat hepatocellular carcinoma. *Colloids and Surfaces B: Biointerfaces*, *204*, p.111778.

38. Mahmoudi, S., Ghorbani, M., Sabzichi, M., Ramezani, F., Hamishehkar, H. and Samadi, N., **2019**. Targeted hyaluronic acid-based lipid nanoparticle for apigenin delivery to induce Nrf2-dependent apoptosis in lung cancer cells. *Journal of Drug Delivery Science and Technology*, *49*, pp.268–276.

39. Zayed, M.M.M., Sahyon, H.A., Hanafy, N.A.N. and El-Kemary, M.A., **2022**. The effect of encapsulated apigenin nanoparticles on HePG-2 cells through regulation of P53. *Pharmaceutics*, *14*(6), p.1160.

40. Esmaeili, F., Ghahremani, M.H., Ostad, S.N., Atyabi, F., Seyedabadi, M., Malekshahi, M.R., Amini, M. and Dinarvand, R., **2008**. Folate-receptor-targeted delivery of docetaxel nanoparticles prepared by PLGA-PEG-folate conjugate. *Journal of Drug Targeting*, *16*(5), pp.415–423.

41. Yoo, H.S. and Park, T.G., **2004**. Folate receptor targeted biodegradable polymeric doxorubicin micelles. *Journal of Control Release*, *96*(2), pp.273–283.

42. Song, X., Zhao, Y., Wu, W., Bi, Y., Cai, Z., Chen, Q., Li, Y. and Hou, S., **2008**. PLGA nanoparticles simultaneously loaded with vincristine sulfate and verapamil hydrochloride: Systematic study of particle size and drug entrapment efficiency. *International Journal of Pharmaceutics*, *350*(1–2), pp.320–329.

43. Tao, Y., Han, J. and Dou, H., **2012**. Surface modification of paclitaxel-loaded polymeric nanoparticles: Evaluation of *in vitro* cellular behavior and *in vivo* pharmacokinetic. *Polymer*, *53*(22), pp.5078–5086.

44. Langer, K., Balthasar, S., Vogel, V., Dinauer, N., Briesen, H.V. and Schubert, D., **2003**. Optimization of the preparation process for human serum albumin (HSA) nanoparticles. *International Journal of Pharmaceutics*, *257*(1–2), pp.169–180.

45. Danaei, M., Dehghankhold, M., Ataei, S., Hasanzadeh Davarani, F., Javanmard, R., Dokhani, A., Khorasani, S. and Mozafari, M.R. **2018**. Impact of particle size and polydispersity index on the clinical applications of lipidic nanocarrier systems. *Pharmaceutics*, *10*(2), p.57.

46. Patel, A., Carpentier, R., Becart, E., Mordacq, G., Betbeder, D. and Nesslany, F., **2016**. Influence of the surface charge of PLGA nanoparticles on their in vitro genotoxicity, cytotoxicity, ROS production and endocytosis. *Journal of Applied Toxicology*, *36*(3), pp.434–444.

47. Honary, S. and Zahir, F., **2013**. Effect of zeta potential on the properties of nano–drug delivery systems–a review (part 1). *Tropical Journal of Pharmaceutical Research*, *12*, pp.255–264.

48. Weiss, B., Schaefer, U.F., Zapp, J., Lamprecht, A., Stallmach, A. and Lehr, C.M., **2006**. Nanoparticles made of fluorescence-labelled poly(l-lactide-co-glycolide): Preparation, stability, and biocompatibility. *Journal of Nanoscience and Nanotechnology*, *6*(9–10), pp.3048–3056.

49. Sen, R., Ganguly, S., Ganguly, S., Debnath, M.C., Chakraborty, S., Mukherjee, B. and Chattopadhyay, D., **2021**. Apigenin-loaded PLGA-DMSA nanoparticles: A novel strategy to treat melanoma lung metastasis. *Molecular Pharmaceutics*, *18*, pp.1920–1938.

50. Zhang, Z., Lee, S.H. and Feng, S.S., **2007**. Folate-decorated poly(lactide-co-glycolide)-vitamin E TPGS nanoparticles for targeted drug delivery. *Biomaterials*, *28*(10), pp.1889–1899.

51. Huang, Y., Mao, K., Zhang, B. and Zhao, Y., **2017**. Superparamagnetic iron oxide nanoparticles conjugated with folic acid for dual target-specific drug delivery and MRI in cancer theranostics. *Materials Science & Engineering C, Materials for Biological Applications*, *70*(Pt 1), pp.763–771.

52. Zeng, L., Luo, L., Pan, Y., Luo, S., Lu, G. and Wu, A., **2015**. In vivo targeted magnetic resonance imaging and visualized photodynamic therapy in deep-tissue cancers using folic acid functionalized superparamagnetic upconversion nanocomposites. *Nanoscale*, *7*, pp.8946–8954.